

Synthesis of ZnO microstructures in glycerol/water solution

Xiaobin Dong, Aiyu Zhang, Ping Yang*

School of Material Science and Engineering, University of Jinan 250022 Jinan, PR China

Received 25 April 2013; received in revised form 30 May 2013; accepted 30 May 2013

Available online 5 June 2013

Abstract

Zinc oxide (ZnO) microrods with high aspect ratio and microstructures with flowerlike morphologies have been synthesized successfully in a glycerol/water reaction system by a simple solvothermal method without adding any surfactants or templates at 180 °C. Experimental results indicated that the flowerlike ZnO microstructures were transformed into rodlike ones with increasing amounts of zinc acetate dihydrate ($\text{Zn}(\text{Ac})_2 \cdot 2\text{H}_2\text{O}$) and sodium hydroxide (NaOH) because of the rapid nucleation and growth, indicating that the concentration of reactants is the key to control the morphologies of ZnO samples. In contrast, double-columned and double-hemisphered ZnO microstructures were fabricated using similar solvothermal conditions without adding NaOH by adjusting the proportion of glycerol and water, for these crystallites were generated mainly by esterification between $\text{Zn}(\text{Ac})_2 \cdot 2\text{H}_2\text{O}$ and glycerol. Time-dependent experiments have also been conducted to explore the evolution of ZnO morphologies. The growth mechanism of as-prepared ZnO structures synthesized in different conditions was discussed.

© 2013 Elsevier Ltd and Techna Group S.r.l. All rights reserved.

Keywords: ZnO; Microstructures; Solvothermal; Morphology

1. Introduction

In the wake of the progress of researches in semiconductor materials, a lot of the unique physical and chemical properties, which can be ascribed to the morphology, grain size, growth orientation and dimensions, were discovered during the past decades, indicating that they have great use in many fields, such as renewable energy [1], nanodevices [2], and so on. Among these materials, zinc oxide (ZnO), a very important wide-band-gap (3.37 eV) metal oxide semiconductor with large exciton binding energy (60 meV) at room temperature [3], has drawn the attention of many researchers due to its superior electronic, chemical and optical properties, and was found quite useful in ultraviolet (UV) lasers [4], chemical sensors [5], piezoelectric devices [6], and solar cells [7–10]. All these attractive applications of ZnO have triggered tremendous interests among people in developing various methods, which include thermal evaporation [11,12], chemical vapor deposition [13,14], electrochemical deposition [15], and wet chemical processes [16–18], to selectively synthesize

various morphologies and control their growth processes for better practical use. Compared with vapor approaches, facile solution methods are considered more convenient and powerful owing to their advantages of simple equipment, low cost, relative low temperature, and their potential for scale-up [19,20].

Among those solution techniques, the solvothermal method is a fashionable route at present, largely because it allows for the synthesis of many different morphologies with various organic reagents, which often is regarded as a structure-directing agent by being incorporated with some functional groups on the surface of nanostructured materials [21]. Pal and Santiago have reported the controlled synthesis of ZnO nanostructures with different morphologies using ethylenediamine by a simple low-temperature hydrothermal technique [22]. Wang et al. have fabricated ZnO with diverse morphologies via an ethanolamine-assisted solvothermal process, and the flowerlike ZnO nanostructures show higher catalytic activity than others [23]. Gao et al. have synthesized porous ZnO hollow spheres whose average crystallite size, shell thickness, and pore structures could be controlled by varying the molar ratio of glucose to zinc ions via a solvothermal process [24]. All these studies are capable of forming various ZnO nanostructures and controlling over the size by changing parameters, including the temperature, time, and

*Corresponding author. Tel.: +86 531 89736225; fax: +86 531 87974453.

E-mail addresses: mse_yangp@ujn.edu.cn,
pyangaist@yahoo.com (P. Yang).

the composition of the reaction mixture. To date, however, the synthesis of ZnO microstructures with specific morphologies and precise sizes remains a challenge, and there are few study in which glycerol has been used to fabricate ZnO microstructures.

In this article, we report a tunable synthesis of ZnO with different morphologies via a simple solvothermal method in a glycerol/water reaction system without adding any surfactants or templates at 180 °C. Rodlike and flowerlike ZnO microstructures were obtained in a mixed solution using NaOH by means of adjusting the concentration of reactants, while double-columned and double-hemisphered ZnO structures were fabricated under the similar solvothermal condition without NaOH through controlling the proportion of glycerol and water. The apparent differences of ZnO microstructures obtained with or without NaOH have demonstrated that the reaction mechanisms in the two similar conditions are obviously distinguished from each other, which means NaOH plays a distinct role in the reactions. On the basis of the experimental results, the possible growth mechanisms of these different ZnO morphologies are discussed in some detail in this paper.

2. Experimental section

2.1. Experimental

Zinc acetate dihydrate ($\text{Zn}(\text{Ac})_2 \cdot 2\text{H}_2\text{O}$, 99%), sodium hydroxide (NaOH, 99%) and glycerol ($\text{C}_3\text{H}_8\text{O}_3$, 99%) were purchased from Sinopharm Chemical Reagent Co. Ltd. All chemicals were of analytical grade and utilized without further purification. Water used for experiments was supplied by a Millipore system ($18.2 \text{ M}\Omega \text{ cm}^{-1}$).

For the synthesis of rodlike and flowerlike ZnO microstructures, $\text{Zn}(\text{Ac})_2 \cdot 2\text{H}_2\text{O}$ and NaOH, whose molar ratio is 1:25, were dissolved in deionized water with stirring to form a clear solution and then glycerol was added to the solution. After 10 min of stirring, the mixture was transferred into a Teflon-lined stainless-steel autoclave with a filling capacity of 50 ml. The autoclave was sealed and maintained at 180 °C for 24 h. Finally, the system was cooled down to room

temperature naturally. The precipitate was collected by centrifugation, washed for several times using water and ethanol to remove unreacted chemicals, and dried in air at 60 °C. To investigate the effect of the concentration of reactants, the amount of NaOH and $\text{Zn}(\text{Ac})_2 \cdot 2\text{H}_2\text{O}$ were changed at a fixed molar ratio, and the proportion of solvents have varied to illustrate the role of glycerol in this reaction. Detailed preparation conditions were summarized in Table 1. Double-columned and double-hemisphered ZnO structures were fabricated under the similar solvothermal process without NaOH. The influences of the amount of $\text{Zn}(\text{Ac})_2 \cdot 2\text{H}_2\text{O}$ and the proportion of solvents on morphology were also explored in this reaction, the detailed conditions of which could be found in Table 1.

2.2. Characterizations

The crystalline structure of samples was characterized by X-ray diffraction (XRD) with a D8 Advance Bruker X-ray diffractometer using a Cu K α target. XRD patterns were recorded from 10° to 80° (2 θ) with a scanning step of 0.02°. The morphologies and sizes of as-prepared samples were examined by a field emission scanning electron microscope (FESEM, FEI, QUANTA FEG 250, United States) and a fluorescence microscope (OLYMPUS, IX81, Japan). Powder samples obtained by a solvothermal process were dispersed in anhydrous ethanol, then dropped on a aluminum foil and dried in air for SEM observation. The Fourier transform infrared (FTIR) spectra of samples were tested by a FTIR spectrometer (Thermo Electron, Nicolet 380, United States).

3. Results and discussion

3.1. Growth mechanism of ZnO microstructures with various morphologies

In the present study, the morphology and size of as-synthesized ZnO samples can be facilely tuned by changing the composition and concentration of reactants as well as the molar ratio of glycerol and water, while the reaction temperature, time and total volume of the solvents remain unchanged.

Table 1
Preparation conditions of ZnO products synthesized in glycerol/water mixture.

Sample	$\text{ZnAc}_2 \cdot 2\text{H}_2\text{O}$ (mmol)	NaOH (mmol)	Glycerol (ml)	H_2O (ml)	Temperature (°C)	Time (h)
1	0.25	6.25	8	7	180	24
2	0.5	12.5	8	7	180	24
3	0.75	18.75	8	7	180	24
4	1	25	8	7	180	24
5	1.5	37.5	8	7	180	24
6	1	25	11	4	180	24
7	1	25	6	9	180	24
8	0.5	–	8	7	180	24
9	1	–	8	7	180	24
10	1.5	–	8	7	180	24
11	1	–	11	4	180	24
12	1	–	6	9	180	24

A series of experiments were performed by varying the precursor concentration but keeping the molar ratio constant between the zinc salt and NaOH. Fig. 1a,b shows typical SEM images of sample 1 synthesized with 0.25 mmol $\text{Zn}(\text{Ac})_2 \cdot 2\text{H}_2\text{O}$ and 6.25 mmol NaOH in the mixture of 8 ml glycerol and 7 ml water. The low magnification SEM image (Fig. 1a) demonstrates that this sample consists of a lot of well-dispersed flowerlike structures. The size of the flowerlike structure is on the scale of micrometers with a diameter of about 2–3 μm . From the high magnification SEM image (Fig. 1b), it can be seen that the surface of each petal in the flowerlike structure is quite rough and the petal seems to be composed of many fused nanorods. Moreover, most of the integrated flowerlike structures have obvious hexagonal symmetry. To confirm the formation of ZnO during this solvothermal process, the phase structure and the composition of the sample were investigated by the XRD pattern shown in Fig. 2. All diffraction peaks can be indexed as hexagonal wurtzite-type ZnO (JCPDS no. 36-1451), and no characteristic peaks of other impurities are detected in the pattern. Besides, the sharp diffraction peaks also indicate the good crystallinity of the prepared crystals. Distinct flowerlike crystals have been fabricated with $\text{Zn}(\text{Ac})_2 \cdot 2\text{H}_2\text{O}$ and NaOH increasing to 0.5 mmol and 15 mmol respectively, as shown in Fig. 1c,d. This flowerlike structure is approximately 5–6 μm in size, consisting of short pencil-like crystals radiating from the center. The diameter of the pencil-like crystals is in the range of 300–900 nm and their length is about 1.5–2.5 μm . Apparent hexagonal symmetry can also be observed in this kind of flowerlike structures. When the amounts of $\text{Zn}(\text{Ac})_2 \cdot 2\text{H}_2\text{O}$ and NaOH were increased to 0.75 mmol and 18.75 mmol separately, the as-obtained products were the mixture of only a few flowerlike structures and many dispersed pencil-like microrods, according to Fig. 1e. The length of these microrods is between 7 and 15 μm and the average diameter is around

1 μm . As shown in Fig. 1f, the flowerlike structure possessing hexagonal symmetrical characteristic is made of some pencil-like crystals with the similar size of those dispersed microrods, which indicates that the dispersed microrods may be derived from the disintegration of the flowerlike structures. It can be indicated from the hexagonal cross sections of the microrods that these products are hexagonal wurtzite-type ZnO [25] and this point has been proved by XRD pattern b of this sample in Fig. 2. Compared with the XRD patterns of sample 1, the diffraction peaks of sample 3 are much sharper, reflecting better crystallinity of the prepared crystals. Furthermore, it is noticeable that the ratios of relative XRD intensities of (100)/(101) are different between the pattern a and pattern b as the amounts of $\text{Zn}(\text{Ac})_2 \cdot 2\text{H}_2\text{O}$ and NaOH increased [26], which would be caused by the different degrees of preferred growth orientation along the *c*-axis of the hexagonal ZnO crystals. With 1 mmol $\text{Zn}(\text{Ac})_2 \cdot 2\text{H}_2\text{O}$ and 25 mmol NaOH, a large

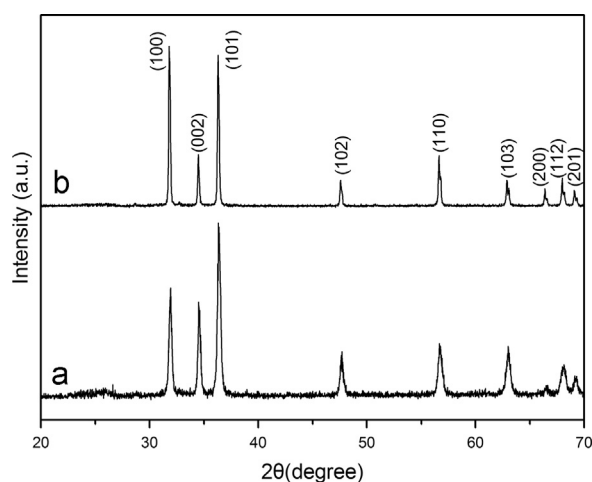


Fig. 2. XRD patterns of (a) sample 1 and (b) sample 3.

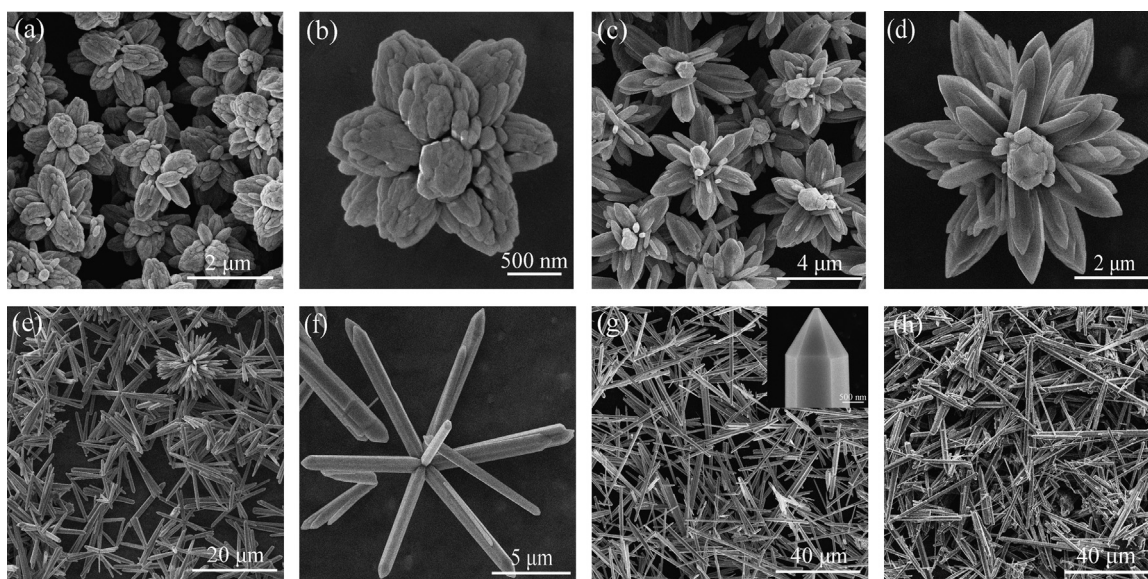


Fig. 1. SEM images of as-prepared ZnO samples synthesized with different concentration of reactants in glycerol/water mixture contained NaOH: (a,b) sample 1, (c,d) sample 2, (e,f) sample 3, (g) sample 4, and (h) sample 5.

quantity of randomly distributed hexagonal ZnO microrods were observed, as shown in Fig. 1g. The diameter of these microrods varies from 1 μm to 2 μm while their length is in the range of 30–60 μm . Thus, in the best case, aspect ratios of some microrods could be close to 35. Besides, in terms of the inset in Fig. 1g, each rodlike ZnO structure has a sharp tip and smooth surfaces. When the amounts of $\text{Zn}(\text{Ac})_2 \cdot 2\text{H}_2\text{O}$ and NaOH were further increased to 1.5 mmol and 37.5 mmol respectively, rodlike ZnO crystals with nonuniform sizes were found in this sample according to Fig. 1h. Though the average diameter of these microrods increases in comparison with products in sample 4, their length does not change a lot, and even has some decreases. On the whole, it can be seen from the morphological study that different amounts of reactants are essential to the formation of ZnO structures under this condition.

To investigate the influence of the proportion of solvents on ZnO structures' morphologies, the other three experiments were conducted utilizing different amounts of glycerol and water. Fig. 3a displays the microphotograph of sample 6 prepared in the mixture of 11 ml glycerol and 4 ml water with 1 mmol $\text{Zn}(\text{Ac})_2 \cdot 2\text{H}_2\text{O}$ and 25 mmol NaOH. The average diameter of these dispersed rodlike ZnO structures is about 500 nm, and the length of them varies from 20 μm to 40 μm . As shown in Fig. 3b (and Fig. 1g), both diameter and length of rodlike ZnO crystals increased in the case of altering volume ratio of glycerol/water from 11/4 to 8/7. When the volume ratio was adjusted to 6/9, ZnO microrods with 1–1.5 μm diameter and 40–80 μm length were observed as shown in Fig. 3c. Though the size of these ZnO structures increases as the volume of glycerol decreases, the morphology remains unchanged in the reaction. That indicates glycerol can only control the size of ZnO crystals, for the mobility and the diffusion length of the ions in the mixed solution are rather limited by its high viscosity. Therefore, compared to the proportion of solvents, the concentration of reactants is much more important to control morphologies of ZnO structures in this process.

On the basis of above morphological study, the formation mechanisms of these ZnO products prepared with NaOH in glycerol/water mixture are probably as follows. Due to the high molar ratio of NaOH and $\text{Zn}(\text{Ac})_2 \cdot 2\text{H}_2\text{O}$ (25:1), a large amount of growth units, $\text{Zn}(\text{OH})_4^{2-}$ complexes, can be generated in the solution rapidly. It has been demonstrated that ZnO

is an unusual inorganic compound that readily forms fourlings when it nucleates. These structures consist of four *c*-axis oriented acicular spines united at a common base and approximately tetrahedral to each other [27]. Since the idealized fourling structure can have many deviations, it is possible that the initial ZnO crystal has many polar (0001) surfaces which have relatively high surface energy [28]. Thus, once the nuclei form in the solution, ZnO crystals will grow from polar (0001) surfaces and spines because of the trend to minimize the total surface energy. Owing to natural hexagonal structure of ZnO, these petals may gradually develop along the six symmetric directions and merge into six larger ZnO crystals, resulting in the fabrication of flowerlike ZnO structures with hexagonal symmetry. As the concentration of the reactants increases, some ZnO petals will grow rapidly from the central nuclei and then limit the growing space of other petals, which cause the number of petal to decrease. In addition, NaOH with high concentration can react with the as-prepared ZnO to form soluble $\text{Zn}(\text{OH})_4^{2-}$ complexes by a inverse process. This would easily lead to the disintegration of the flowerlike crystals, since these structures' centers possessing many deviations have relative high energy. Based on above two reasons, many rodlike ZnO were obtained in samples 3–5. Furthermore, it is worth noting that most ZnO petals and rods prepared in our study have sharp tips, which have been reported and explained extensively in previous literature [29,30].

3.2. Morphologies and growth mechanism of ZnO products synthesized in glycerol/water mixture without NaOH

In this condition, the effect of the concentration of Zn $(\text{Ac})_2 \cdot 2\text{H}_2\text{O}$ on morphology remains to be studied first. Fig. 4 shows the microphotographs of as-prepared ZnO samples synthesized with different amount of $\text{Zn}(\text{Ac})_2 \cdot 2\text{H}_2\text{O}$ in the mixture of 8 ml glycerol and 7 ml water. Different from the morphology of sample 4 synthesized in the solution contained NaOH, some rodlike and double-columned structures with low aspect ratio were obtained with 1 mmol $\text{Zn}(\text{Ac})_2 \cdot 2\text{H}_2\text{O}$ in this reaction, as shown in Fig. 4b. Each double-columned structure consists of two parts united at a common base, and they are shorter but thicker than most of those rodlike crystals. The obtained rods are

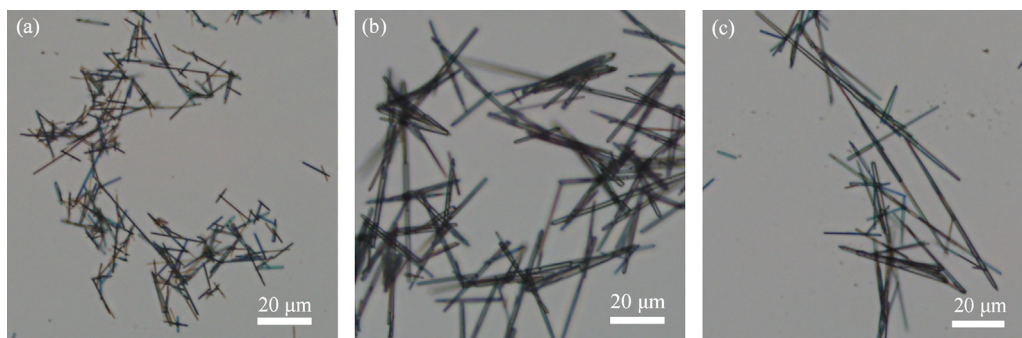


Fig. 3. Microphotographs of as-prepared ZnO samples synthesized with different proportion of solvents in glycerol/water mixture containing NaOH: (a) sample 6, (b) sample 4, and (c) sample 7.

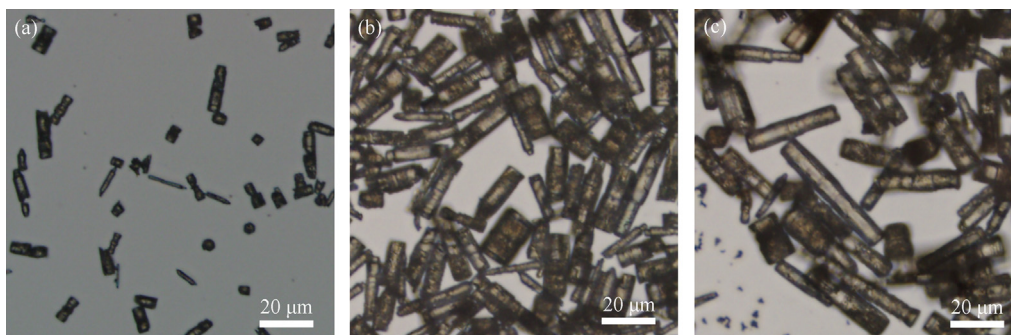


Fig. 4. Microphotographs of as-prepared ZnO samples synthesized with different amount of $\text{Zn}(\text{Ac})_2 \cdot 2\text{H}_2\text{O}$ in glycerol/water mixture: (a) sample 8, (b) sample 9, and (c) sample 10.

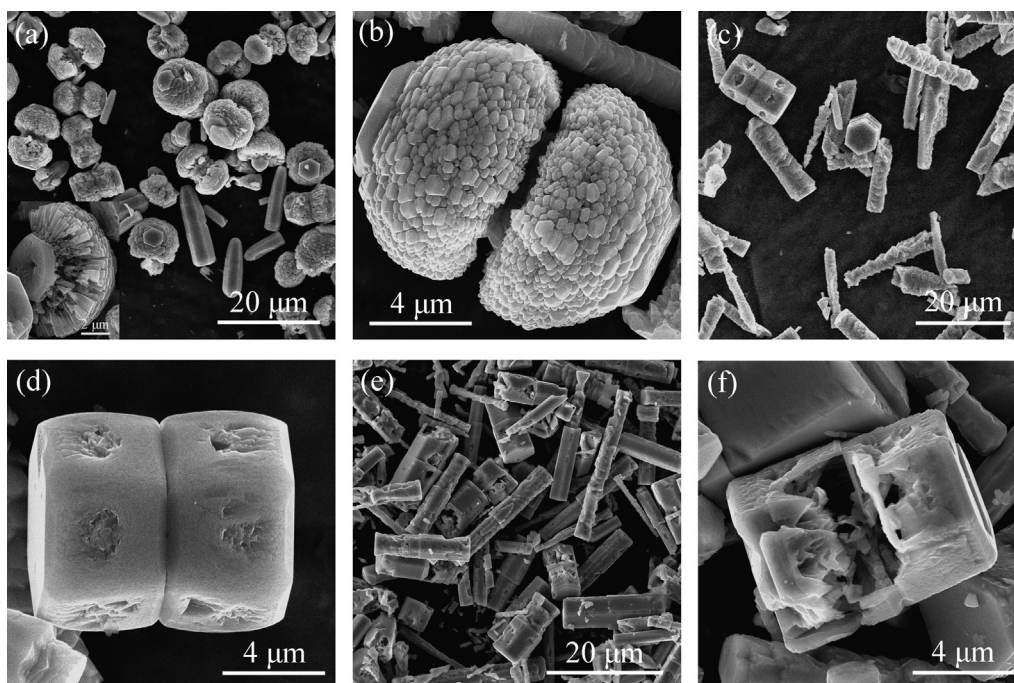


Fig. 5. SEM images of as-prepared ZnO samples synthesized with different proportion of solvents in glycerol/water mixture: (a,b) sample 11, (c,d) sample 9, and (e,f) sample 12.

about 4–7 μm in diameter and 20–40 μm in length. As shown in Fig. 4a, when the amount of $\text{Zn}(\text{Ac})_2 \cdot 2\text{H}_2\text{O}$ were decreased to 0.5 mmol, the size of rodlike and double-columned structures all reduced. And when the amount of $\text{Zn}(\text{Ac})_2 \cdot 2\text{H}_2\text{O}$ were increased to 1.5 mmol, the morphology of as-prepared products remained unchanged except that the rodlike structures had a little increase in size according to Fig. 4c. Hence, it can be deduced from Fig. 4 that the precursor concentration does not play a major role in controlling morphology in this condition.

To further observe the morphology of sample 9, the synthesized products were characterized by SEM, as shown in Fig. 5c and d. The SEM image with low magnification (Fig. 5c) demonstrates that the surfaces of these rodlike structures are quite rough and obvious defects can be observed in double-columned structures. Fig. 5d gives a clearer show of the double-columned structures. Some irregular pits, even small cavities, appear in the side facets of the two columns symmetrically, and

the cross section of the columns is hexagonal. The XRD pattern of this sample in Fig. 6 displays no characteristic peaks of impurities, suggesting that both rodlike structures and double-columned structures are hexagonal wurtzite-type ZnO. In spite of the rough surfaces and defects in the crystals, the sharp shape and line widths of the diffraction peaks indicate they have excellent crystallinity. When the volume ratio of glycerol/water was adjusted from 8/7 to 11/4, many double-hemisphered and some rodlike structures were formed in sample 11, according to Fig. 5a. As the name implies, double-hemisphered structure is composed of two hemispheres growing at a base in between. Besides, a hexagonal plane is found at the top of each hemisphere. The inset in Fig. 5a shows a separated hemisphere, from which it can be clearly seen that a lot of nanorods radiate from the center and the base of the double-hemisphered structure is hexagonal likewise. Therefore, we think this distinct structure may be derived from double-columned structure, and

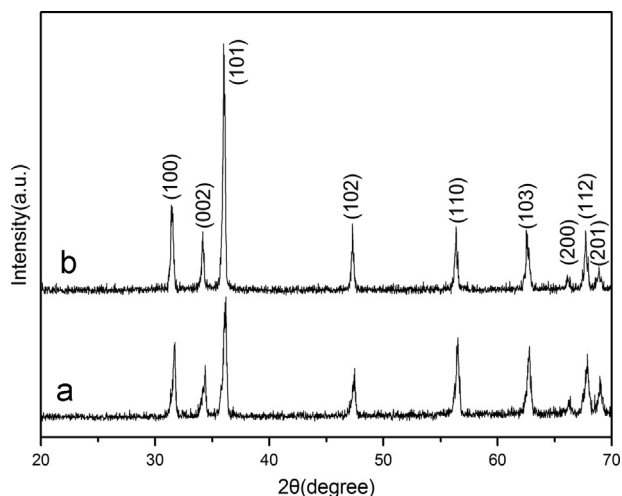


Fig. 6. XRD patterns of sample 11 (a) and sample 9 (b).

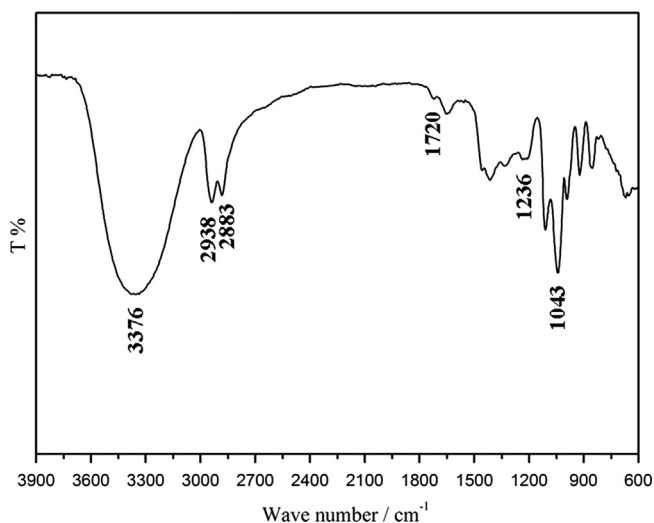
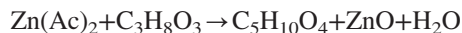


Fig. 7. FTIR spectrum of sample 9.

then many nanorods grow around the side facets of the two columns. The high magnification SEM image (Fig. 5b) reveals that every nanorod has hexagonal cross section, indicating their preferred growth along the *c*-axis of the hexagonal ZnO. The XRD pattern of sample 11 in Fig. 6 has proved that these crystals are hexagonal wurtzite-type ZnO with good crystallinity. In the case of altering volume ratio of glycerol/water from 8/7 to 6/9, the double-columned and rodlike structures with more defects were obtained, as shown in Fig. 5e. Compared with crystals in sample 9, both of these two kinds of structures have a certain degree of increase in length. At the same time, the surfaces of rodlike structures get rougher and obvious holes can be observed in double-columned ZnO according to Fig. 5f, which all lead to the formation of some small particles distributed in the sample. Based on the morphological variation shown in Fig. 5, the volume ratio of glycerol/water is supposed to have major influence on controlling morphologies of ZnO structures in this process.

The evident distinction of the factors affecting the ZnO morphologies in the two different conditions should be caused

by different reaction mechanisms. Without the addition of NaOH, $\text{Zn}(\text{OH})_4^{2-}$ cannot be generated as growth unit. Thus these ZnO structures are synthesized mainly by esterification between zinc acetate and glycerol in the process, which is similar to the reaction mechanism proposed in a previous paper [31]. The whole reaction can be expressed as follows:



$\text{C}_5\text{H}_{10}\text{O}_4$ here refers to glyceryl monoacetate. This mechanism was testified by the evidence that the ester group is present in the finished reaction liquid of sample 9, according to the FTIR spectrum shown in Fig. 7. The strong absorption peak at 1043 cm^{-1} can be indexed to the C–O–C symmetric stretch vibration while the absorption peak at 1236 cm^{-1} is the unsymmetric stretch vibration of C–O–C. The weak absorption at 1720 cm^{-1} is attributed to the typical absorption of C=O. These peaks all prove the generation of ester group. The absorption peaks at 2938 cm^{-1} and 2883 cm^{-1} are relevant to the stretch vibration of $-\text{CH}_2-$ and the broad peak centered at 3376 cm^{-1} is in accordance with the typical absorption of $-\text{OH}$, which indicates the existence of unreacted glycerol. Furthermore, when zinc source was changed into ZnCl_2 or $\text{Zn}(\text{NO}_3)_2$, no ZnO crystals were obtained in this reaction, implying that CH_3COO^- plays a significant role in synthesizing ZnO. In addition, it should be pointed out that esterification generally needs the catalysis of H^+ , and thus the reaction environment contained NaOH may intensively suppress the occurrence of this reaction.

In order to reveal the formation mechanism of ZnO in this condition, time-dependent experiments of sample 9 were conducted to get insight into the evolution process. The products collected at different reaction time are shown in Fig. 8. At the early stage of 0.5 h (Fig. 8a), plenty of double-columned ZnO crystals with uniform size are formed and both length and diameter of this structure are about $5.5\text{ }\mu\text{m}$. When the reaction time is prolonged to 1.5 h (Fig. 8b), the size of double-columned structures obviously increases. The length of most products is between 12 and $17\text{ }\mu\text{m}$ and the average diameter is around $9\text{ }\mu\text{m}$. Besides, a few of long double-columned crystals are also found in the sample, and their bases become vague. By increasing the time to 6 h (Fig. 8c), a lot of rodlike structures with average diameter of $3\text{ }\mu\text{m}$ and various length are obtained, whereas the size of double-columned structures have no big change. Compared with the products in Fig. 8b, black shadow in the crystals can be seen from this sample, which corresponds to the rough surfaces and defects in the SEM images of sample 9. As the reaction time increases to 12 h (Fig. 8d), the mean diameters of rodlike and double-columned structures both have a little decrease. At the same time, the color of the black shadow gets deeper, indicating rougher surfaces and more defects in these crystals.

According to above experimental facts, a schematic diagram, depicted in Fig. 9, has been proposed to illustrate the formation mechanism of the ZnO structures in this reaction. At the early stage, OH^- is obtained by esterification between CH_3COO^- and glycerol while glyceryl monoacetate ($\text{C}_5\text{H}_{10}\text{O}_4$) is generated at the same time. It is well known that glyceride is often used as

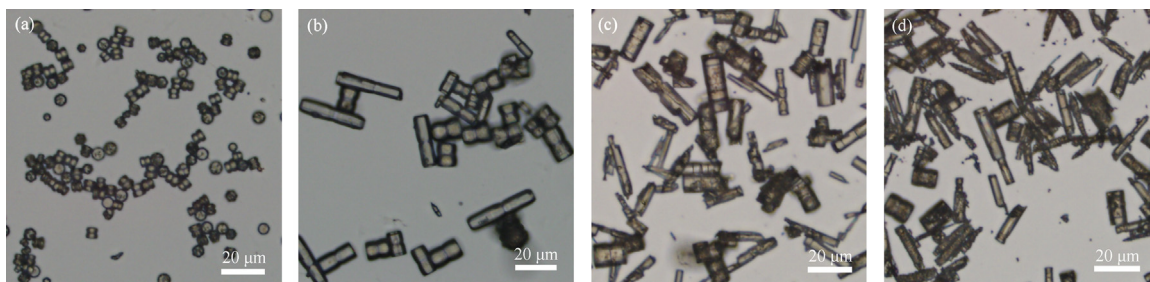


Fig. 8. Microphotographs of the products obtained with different reaction time: (a) 0.5 h, (b) 1.5 h, (c) 6 h, and (d) 12 h.

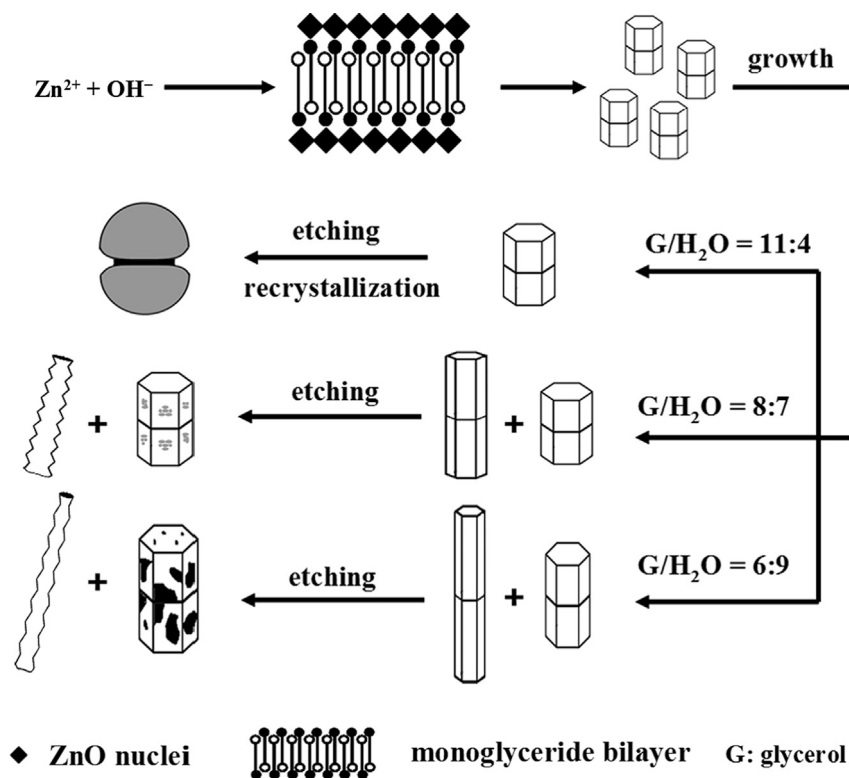


Fig. 9. Schematic illustration of the evolution process of obtained ZnO structures in the process without NaOH.

nonionic surfactant and micelle will be formed when the concentration of the surfactant reaches CMC (critical micelle concentration). Thus we consider the obtained glyceryl monoacetate can be regarded as a surfactant and it may form the bilayer micelle in this condition. Because the concentration of the glyceryl monoacetate depends on the amount of $\text{Zn}(\text{Ac})_2$, which is a constant value, bilayer micelle could be generated in the reactions with different volume ratios of glycerol/water. Due to the relative low nucleation barrier, ZnO tends to nucleate at two sides of bilayer micelle. After a continuous growth, two columns would be obtained on both sides of the micelle and then the organic molecules could be expelled gradually [32], resulting in the formation of double-columned ZnO structures with uniform size. Afterward, these crystals continue to develop to bigger size and some long double-columned products would be observed when volume ratios of glycerol/water are 8/7 and 6/9. This is because the relative low viscosity in the two conditions does not limit the mobility and the diffusion length of the ions, which is

favorable of the preferred growth of ZnO along its c -axis. The growth of ZnO structures will stop at a certain time as Zn^{2+} is exhausted, and then water is likely to be an etching agent to further change the morphologies of these crystals. At high temperature, ionization balance of water ($\text{H}_2\text{O} \leftrightarrow \text{H}^+ + \text{OH}^-$) will move right, implying that the concentration of H^+ increases. Owing to the reaction between ZnO and H^+ , some long double-columned products will rupture at the common base to form many rodlike ZnO structures, and plenty of defects as well as rough surfaces appear in these ZnO crystals. Likewise, this reaction can explain why crystals in sample 12 have more defects than that in sample 9 during the same period of time. When volume ratio of glycerol/water becomes 11/4, double-hemispherical structures are obtained, which may be ascribed to the recrystallization of the etched ZnO around the double-columned products' side facets. Further study is needed to clarify this point of view. In addition, it should be pointed out that NaOH could intensively suppress the ionization of water, and

thus almost no defects are found in the crystals synthesized by the reaction with NaOH.

4. Conclusion

In summary, ZnO with different morphologies have been synthesized via the simple solvothermal method in a glycerol/water system. Rodlike and several kind of flowerlike ZnO structures were obtained using NaOH by means of adjusting the concentration of reactants, while double-columned and double-hemisphered ZnO crystals were fabricated under the similar solvothermal condition without NaOH through controlling the proportion of glycerol and water. Experimental facts have demonstrated that the formation mechanisms of the ZnO structures obtained with or without NaOH are totally different from each other, and glycerol also plays distinct roles in the two conditions. Since the process is well repeatable and can give a high yield of the products, our study may provide a potential method for the controllable syntheses of other semiconductors with novel morphologies.

Acknowledgments

This work was supported by the Program for Taishan Scholars from Shandong Province Government, projects from the National Natural Science Foundation of China (21071061), the Shandong Provincial Natural Science Foundation, China (ZR2010EZ001), and the Outstanding Young Scientists Foundation Grant of Shandong Province (BS2010CL004 and BS2012CL006).

References

- [1] Meng Ni, Michael K.H. Leung, Dennis Y.C. Leung, K. Sumathy, A review and recent developments in photocatalytic water-splitting using TiO_2 for hydrogen production, *Renewable and Sustainable Energy Reviews* 11 (2007) 401–425.
- [2] Z.L. Wang, Nanobelts, nanowires, and nanodiskettes of semiconducting oxides—from materials to nanodevices, *Advanced Materials* 15 (2003) 432–436.
- [3] Yi Wang, Meng Li, Hydrothermal synthesis of single-crystalline hexagonal prism ZnO nanorods, *Materials Letters* 60 (2006) 266–269.
- [4] M.H. Huang, S. Mao, H. Feick, H. Yan, Y. Wu, H. Kind, E. Weber, R. Russo, P. Yang, Room-temperature ultraviolet nanowire nanolasers, *Science* 292 (2001) 1897–1899.
- [5] J. Huang, Y. Wu, C. Gu, M. Zhai, Y. Sun, J. Liu, Fabrication and gas-sensing properties of hierarchically porous ZnO architectures, *Sensors and Actuators B* 155 (2011) 126–133.
- [6] Z.L. Wang, J.H. Song, Piezoelectric nanogenerators based on zinc oxide nanowire arrays, *Science* 312 (2006) 242–246.
- [7] C. Zhu, X. Pan, C. Ye, L. Wang, Z. Ye, J. Huang, Effect of CdSe quantum dots on the performance of hybrid solar cells based on ZnO nanorod arrays, *Ceramics International* 39 (2013) 2975–2980.
- [8] L. Luo, W. Tao, X. Hu, T. Xiao, B. Heng, W. Huang, H. Wang, H. Han, Q. Jiang, J. Wang, Y. Tang, Mesoporous F-doped ZnO prism arrays with significantly enhanced photovoltaic performance for dye-sensitized solar cells, *Journal of Power Sources* 196 (2011) 10518–10525.
- [9] M. Krunk, A. Katerski, T. Dedova, I. Oja Acik, A. Mere, Nanostructured solar cell based on spray pyrolysis deposited ZnO nanorod array, *Solar Energy Materials and Solar Cells* 92 (2008) 1016–1019.
- [10] Y. Lin, J. Yang, Y. Meng, Nanostructured ZnO thin films by SDS-assisted electrodeposition for dye-sensitized solar cell applications, *Ceramics International* 39 (2013) 5049–5052.
- [11] J. Wu, T. Li, C. Wang, B. Zhu, R. Wu, C. Xie, The sintering characteristics of pure tetrapod ZnO nanopowders prepared by thermal evaporation deposition (TED), *Ceramics International* 37 (2011) 3469–3476.
- [12] Geun-Hyoung Lee, Optimal Zn/O ratio in vapor phase for the synthesis of high quality ZnO tetrapod nanocrystals via thermal evaporation of Zn in air, *Applied Surface Science* 259 (2012) 562–565.
- [13] G.Z. Wang, Y. Wang, M.Y. Yau, C.Y. To, C.J. Deng, Dickon H.L. Ng, Synthesis of ZnO hexagonal columnar pins by chemical vapor deposition, *Materials Letters* 59 (2005) 3870–3875.
- [14] F. Liu, P.J. Cao, H.R. Zhang, C.M. Shen, Z. Wang, J.Q. Li, H.J. Gao, Well-aligned zinc oxide nanorods and nanowires prepared without catalyst, *Journal of Crystal Growth* 274 (2005) 126–131.
- [15] Y.F. Gao, M. Nagai, Y. Masuda, F. Sato, K. Koumoto, Electrochemical deposition of ZnO film and its photoluminescence properties, *Journal of Crystal Growth* 286 (2006) 445–450.
- [16] Narges Kiomarsipour, Reza Shoja Razavi, Hydrothermal synthesis and optical property of scale- and spindle-like ZnO, *Ceramics International* 39 (2013) 813–818.
- [17] Y. Lee, S. Lee, I. Park, Growth of ZnO hemispheres on silicon by a hydrothermal method, *Ceramics International* 39 (2013) 3043–3048.
- [18] Q. Ahsanulhaq, S.H. Kim, J.H. Kim, Y.B. Hahn, Structural properties and growth mechanism of flower-like ZnO structures obtained by simple solution method, *Materials Research Bulletin* 43 (2008) 3483–3489.
- [19] H. Zhang, D.R. Yang, X.Y. Ma, N. Du, J.B. Wu, D.L. Que, Straight and thin ZnO nanorods: hectogram-scale synthesis at low temperature and cathodoluminescence, *Journal of Physical Chemistry B* 110 (2006) 827–830.
- [20] S. Xu, Z.L. Wang, One-dimensional ZnO nanostructures: solution growth and functional properties, *Nano Research* 4 (2011) 1013–1098.
- [21] K. Thongsuriwong, P. Amornpitoksuk, S. Suwanboon, The effect of aminoalcohols (MEA, DEA and TEA) on morphological control of nanocrystalline ZnO powders and its optical properties, *Journal of Physics and Chemistry of Solids* 71 (2010) 730–734.
- [22] U. Pal, P. Santiago, Controlling the morphology of ZnO nanostructures in a low-temperature hydrothermal process, *Journal of Physical Chemistry B* 109 (2005) 15317–15321.
- [23] X. Wang, Q. Zhang, Q. Wan, G. Dai, C. Zhou, B. Zou, Controllable ZnO architectures by ethanolamine-assisted hydrothermal reaction for enhanced photocatalytic activity, *Journal of Physical Chemistry C* 115 (2011) 2769–2775.
- [24] J. Yu, X. Yu, Hydrothermal synthesis and photocatalytic activity of zinc oxide hollow spheres, *Environmental Science & Technology* 42 (2008) 4902–4907.
- [25] H. Wang, T. Wang, X. Wang, R. Liu, B. Wang, H. Wang, Y. Xu, J. Zhang, J. Duan, Double-shelled ZnO/CdSe/CdTe nanocable arrays for photovoltaic applications: microstructure evolution and interfacial energy alignment, *Journal of Materials Chemistry* 22 (2012) 12532–12537.
- [26] Q. Wu, X. Chen, P. Zhang, Y. Han, X. Chen, Y. Yan, S. Li, Amino acid-assisted synthesis of ZnO hierarchical architectures and their novel photocatalytic activities, *Crystal Growth & Design* 8 (2008) 3010–3018.
- [27] R.A. McBride, J.M. Kelly, D.E. McCormack, Growth of well-defined ZnO microparticles by hydroxide ion hydrolysis of zinc salts, *Journal of Materials Chemistry* 13 (2003) 1196–1201.
- [28] S. Cho, H. Jeong, D. Park, S. Jung, H. Kim, K. Lee, The effects of vitamin C on ZnO crystal formation, *CrystEngComm* 12 (2010) 968–976.
- [29] H. Zhang, D. Yang, Y. Ji, X. Ma, J. Xu, D. Que, Low temperature synthesis of flowerlike ZnO nanostructures by cetyltrimethylammonium bromide-assisted hydrothermal process, *Journal of Physical Chemistry B* 108 (2004) 3955–3958.
- [30] R. Shi, P. Yang, J. Wang, A. Zhang, Y. Zhu, Y. Cao, Q. Ma, Growth of flower-like ZnO via surfactant-free hydrothermal synthesis on ITO substrate at low temperature, *CrystEngComm* 14 (2012) 5996–6003.
- [31] H. Du, F. Yuan, S. Huang, J. Li, Y. Zhu, A new reaction to ZnO nanoparticles, *Chemistry Letters* 33 (2004) 770–771.
- [32] K.X. Yao, R. Sinclair, H.C. Zeng, Symmetric linear assembly of hourglass-like ZnO nanostructures, *Journal of Physical Chemistry C* 111 (2007) 2032–2039.